



Design of the high-efficiency transmission-type polarization converter based on substrate-integrated waveguide (SIW) technology

Haiyan Chen¹ · Liandi Han¹ · Rui Zhao¹ · Fengxia Li¹ · Yang Zhou¹ · Zhipeng Zhou² · Xiaoqiu Li² · Xiaolong Weng¹ · Difei Liang³ · Jianliang Xie¹ · Longjiang Deng¹

Received: 5 January 2019 / Accepted: 12 March 2019 / Published online: 18 March 2019
© Springer-Verlag GmbH Germany, part of Springer Nature 2019

Abstract

In this paper, the design of a three-layer linear polarization converter based on substrate-integrated waveguide (SIW) technology is demonstrated. The transmission-type polarization converter with dual frequency polarization conversion characteristics is realized by a square-slot sandwiched by two layers of off-center dipole-slot resonator, and its asymmetric transmission (AT) property can be obtained by rotating the upper and the lower dipole-slot resonator to form an interlaced layout. An excellent polarization conversion ratio (PCR) can be realized by integrating the traditional transmission-type polarization converter with an SIW, and its physical mechanism can be explicated by guided wave field theory. Experimental results are presented and compared with the simulation results, and they demonstrated that ultra-high PCRs of the presented polarization converter are 0.87 and 0.99 for the measurement at the working frequency of 7.34 GHz and the simulation at the working frequency of 7.6 GHz, respectively. The designed polarization converter has greatly expanded the application field of SIW technology.

1 Introduction

Metamaterials (MMs), as an artificial material, have largely been stimulated by the perfect absorber [1, 2, 2], invisibility cloaking [3, 4] and polarization converter [5–9] due to its extraordinary electro-magnetic (EM) properties. In practical applications, it is very important to manipulate the polarization state of an arbitrary incident wave, mainly because of its wide potential utilizations including antennas [10–12], radome [13, 14] and so on [15–18]. Therefore, MMs-based polarization converters have been studied extensively. Considering the innate advantages of experimental and commercial utilization, polarization modulation in transmission

mode is more attractive [19]. Conventional transmission-type polarizer typically operates in narrow frequency bands (about 20% fractional bandwidth) and has low efficiency, but the high performances are usually achieved at the price of more complex structure [20]. Hence, the implementation of transmission-type polarizer with simple structure and low cost has aroused great interests.

More recently, a remarkable progress has been made on the polarization converter devices in wide band and high efficiency. In 2013, Grady [21] brought up a cut-wire array structure that is capable of rotating a linear polarization state into its orthogonal state in the frequency of 0.8–1.9 THz, and the multi-layer design of the cut-wire could realize anomalous refraction in 0.4–1.8 THz. Subsequently, Yijun Feng and others [22, 23] designed an active chiral MM which could dynamically control the asymmetric EM wave transmission at microwave frequencies using planar MM of deep subwavelength thickness incorporated with active components of PIN diodes. In general, the physical mechanisms of the existing polarizer are restricted to the cross-coupling between the electric and magnetic, and the efficiency of polarization conversion is still unsatisfactory.

Substrate-integrated waveguide (SIW) is integrated waveguide-like structure realized using two rows of metal pins or slots embedded in a dielectric substrate that electrically connect two parallel metal plates [24]. SIW structures integrate

✉ Haiyan Chen
chenhy@uestc.edu.cn

¹ National Engineering Research Center of Electromagnetic Radiation Control Materials, State Key Laboratory of Electronic Thin Film and Integrated Devices, University of Electronic Science and Technology of China, 610054 Chengdu, China

² National Key Laboratory of Antenna and Microwave Technology, Nanjing Research Institute of Electronics Technology, 210013 Nanjing, China

³ Chengdu Jia Chi Electronic Technology Co., Ltd, 610041 Chengdu, China

the advantages of traditional transmission line and possess the advantages of conventional metallic waveguides, such as high-quality factor and high power handling capability with self-consistent electrical shielding [25]. Based on the above considerations, SIW technology is expected to solve the technical bottleneck of polarization conversion efficiency improvement. In fact, the idea of SIW technology is derived from waveguide structures. The polarization converters for waveguide systems and horn antennas have been extensively studied [26–30], and their similar advantage lies in high efficiency. Therefore, SIW technology is employed for improving the efficiency of a polarization conversion, which is also the main topic in this paper.

In this work, a three-layer high-efficiency polarization converter based on SIW technology is presented, which could convert y-polarization incident wave to x-polarized transmitted wave with an efficiency of nearly 1.0 at the working frequency of 7.33 GHz. The electromagnetic transmission properties of the proposed structure are analyzed by the finite-difference time-domain (FDTD) method. To validate our design, the designed structure is fabricated using the conventional printed circuit board (PCB) process, and the tests are performed employing free-space method in microwave anechoic chamber. The physical mechanism of the high-efficient cross-polarization conversion for the proposed structure could be explained according to the electromagnetic transmission mode of a traditional metal rectangle waveguide. Besides, based on the surface current distribution and the characteristic of the electrical field mode in SIW cavity, the physical mechanism of high-efficiency transmission can be clarified much further.

2 Physical principle of operation

At first, design method of the imbedded SIW will be discussed in detail. Since the surface current could only flow along the metal cylinder in z-direction, the cavity only supports TM_{mn0} modes ($m=0,1,2,3\dots, n=0,1,2,3\dots$). Furthermore, the appropriate high-order electric field mode should be selected to excite resonance in the cavity. Therefore, based on the Eq. (1) [31, 32], SIW cavity’s resonance frequency f and the geometrical parameters can be accurately confirmed.

$$W = \frac{c_0 \sqrt{m^2 + n^2}}{2f \sqrt{\epsilon_r}} + \frac{D^2}{0.95P} \tag{1}$$

where W is the cavity length, c_0 is the speed of light in vacuum, and ϵ_r is the relative permittivity of the substrate, and the P and D are the period and diameter of the metal cylinders which could be determined by Eq. 2:

$$P < \frac{\lambda_0 \sqrt{\epsilon_r}}{2}, D < P < 2D \tag{2}$$

Based on this physical theory, the preset parameters of the SIW can be obtained according to the technical requirements of polarization converter.

3 Design and analysis

The geometry of the presented SIW-based polarization converter is illustrated in Fig. 1. It consists of three layers of slotted metal integrated with SIW and is sandwiched by two dielectric layers having the same thickness (that is, $t_1 = t_2 = 1.6$ mm), and the period of the unit cell p was set as 20 mm. Figure 1b depicts the front view of the upper slotted metal patch layer, the side length of the slotted metal patch is marked as W ; the length and width of the x-direction slot (its long axis is in x axis) are l_1 and l_2 . The middle layer metal is the square ring patch and its geometrical parameters are l_3 and l_2 . The middle layer metal is square ring patch and its geometrical parameters are l_3 and l_4 as shown in Fig. 1c. The parameters of the lower slotted metal are identical to the upper layer, but the slot is y-direction to convert the incident wave, just as shown in Fig. 1d. The optimized key parameters are as follows: $W = 18.4$ mm, $a = 4.5$ mm, $l_1 = 12$ mm, $l_2 = 1$ mm,

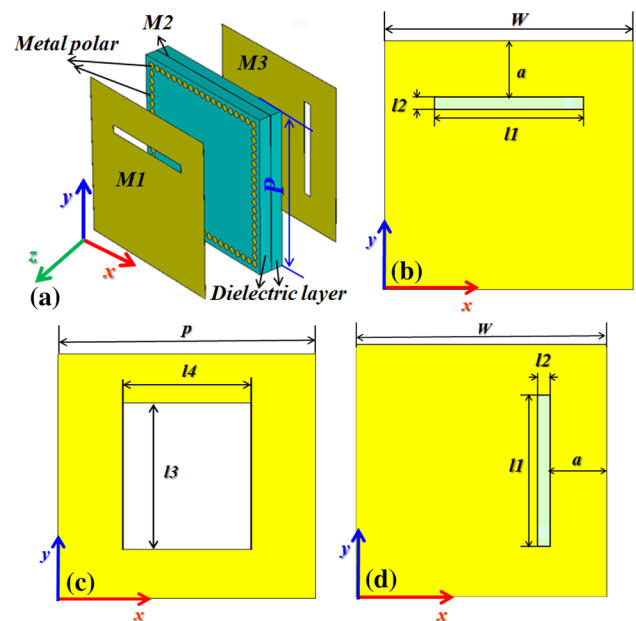


Fig. 1 Schematic diagrams of the designed SIW-based polarization converter. **a** Perspective view of the expanded structure, **b** front view of the structure (marked as M1), **c** the middle layer metal (marked as M2) and **d** the bottom layer meal (marked as M3)

$l_3 = 12$ mm, $l_4 = 10$ mm and the metal is copper with conductivity $= 5.96 \times 10^7$ Sm^{-1} which was fabricated on a Teflon substrate with a permittivity $= 2.1$ and a dielectric loss tangent of 0.0002 . The commercial software CST Microwave Studio [33] and frequency domain solver were employed to simulate the transmission performance of the converter with unit cell boundary condition imposed in the x - y directions and Floquet port in z -direction.

Considering of the polarization of the incident EM waves, we define E_{xi} and E_{yi} to represent the direction of electric field polarization along the x - axis and the y -axis, respectively, just as shown in Fig. 1(a). Therefore, the transmission of y -to- y , y -to- x , x -to- y and x -to- x polarization conversions can be defined as: $t_{yy} = |E_{yt}/E_{yi}|$, $t_{xy} = |E_{xt}/E_{yi}|$, $t_{yx} = |E_{yt}/E_{xi}|$ and $t_{xx} = |E_{xt}/E_{xi}|$, respectively, where t_{yy} and t_{xx} are called the co-polarization transmission, and t_{xy} and t_{yx} are called cross-polarization transmission. In these equations, E denotes the electric field, while the subscripts i and t represent the incidence and transmission of electromagnetic waves.

In Fig. 2, we illustrate the simulated transmission coefficients in the polarization converter for the x -polarization and y -polarization incidence waves under normal incidence. Considering the inherent polarization sensitivity of this designed structure, both the co-polarization transmission t_{xx} and the cross-polarization transmission t_{yx} are zero for the x -polarization incidence waves. Therefore, nearly all the x -polarized incident wave is blocked in this bandwidth. For the y -polarization incidence waves, it can be seen that only cross-polarization transmission coefficient t_{xy} has three resonance peaks at 7.34 GHz, 10.79 GHz and 11.79 GHz with polarization efficiency over 0.8, which means that in these three frequencies, most of the incident

y -polarized wave is converted into x -polarized transmitted electromagnetic wave. Meanwhile, another co-polarization transmission coefficient t_{yy} is almost zero.

The polarization conversion ratio (PCR) is defined as [34]:

$$\text{PCR} = \left(|r_{xy}|^2 + |t_{xy}|^2 \right) / \left(|r_{xy}|^2 + |r_{yy}|^2 + |t_{xy}|^2 + |t_{yy}|^2 \right) \tag{3}$$

Based on the power transmission properties of the designed transmission-type polarization converter, its PCR at the resonant frequency of 7.34 GHz is near 1. Next, we will focus on the physical mechanisms of achieving perfect polarization conversion at the key frequency of 7.34 GHz.

In particular, the cross-polarization transmission coefficient is near 1 at the resonance frequency of 7.34 GHz, which means that the SIW technology is introduced to obtain nearly perfect polarization conversion. Based on the physical theory discussed in Sect. 2, on the basis of Eq. (2), the P and D are chosen as 1 mm and 0.8 mm for exciting the high-order electric field effectively in this paper. Moreover, according to Eq. 1, high-order electric field TM_{120} and TM_{210} are selected, the resonance frequency f can be calculated as about 7.3 GHz. Therefore, the first resonance frequency 7.34 GHz as shown in Fig. 2 coincides well with the calculated one by Eq. (1), which could prove that electric field conversion could be achieved due to the coupling of high-order electric field.

To further investigate the coupling effect in the SIW cavity, the high-order electric field distributions at the resonant frequency of 7.34 GHz are proposed, just as shown in Fig. 3a, b. Obviously, as seen in Fig. 3, we can find that the three-layer structure could form two isolated cavities, TM_{120} can be excited by the y -polarized incident wave in the upper cavity and, subsequently, TM_{120} would convert into TM_{210} mode by the perturbations of the x -direction slot on the bottom metal layer. Thus, due to the coupling of the high-mode electric field, the y -polarized incident wave could be rotated 90° , and y - x polarization conversion can be achieved.

To further clarify the specific changing process of electric field in x - and y -directions, we discuss the electric field distributions at different positions in the wave transmitted direction (that is, in $-z$ direction). Just as shown in Fig. 4, the evolution of the electric fields in the SIW cavity can be clearly observed. For the electric field polarized along the y -direction (that is, y -polarized wave), the electric field distributions are distributed merely in the transverse slot in all the six samples as shown in Fig. 4a-f. Furthermore, when the wave propagates in the structure, the y -component of electric field gradually diminishes as shown in Fig. 4a-f, on the contrary, the x -component progressively increases as shown in Fig. 4g-m. The above analysis shows that a large fraction of incident energy of the y -polarized light gets

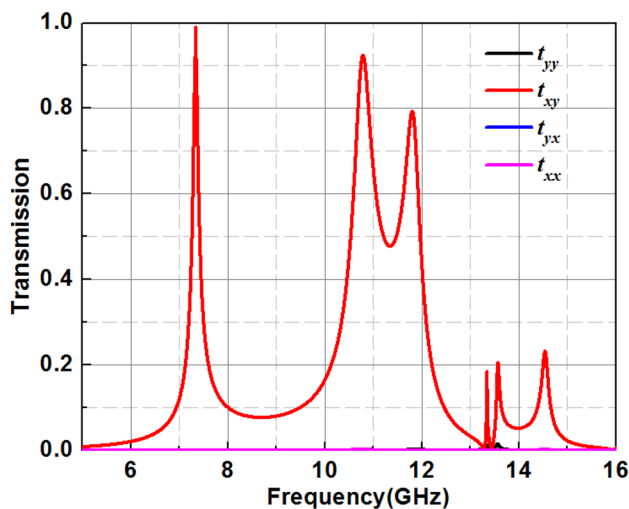


Fig. 2 Transmission properties of the proposed polarization converter

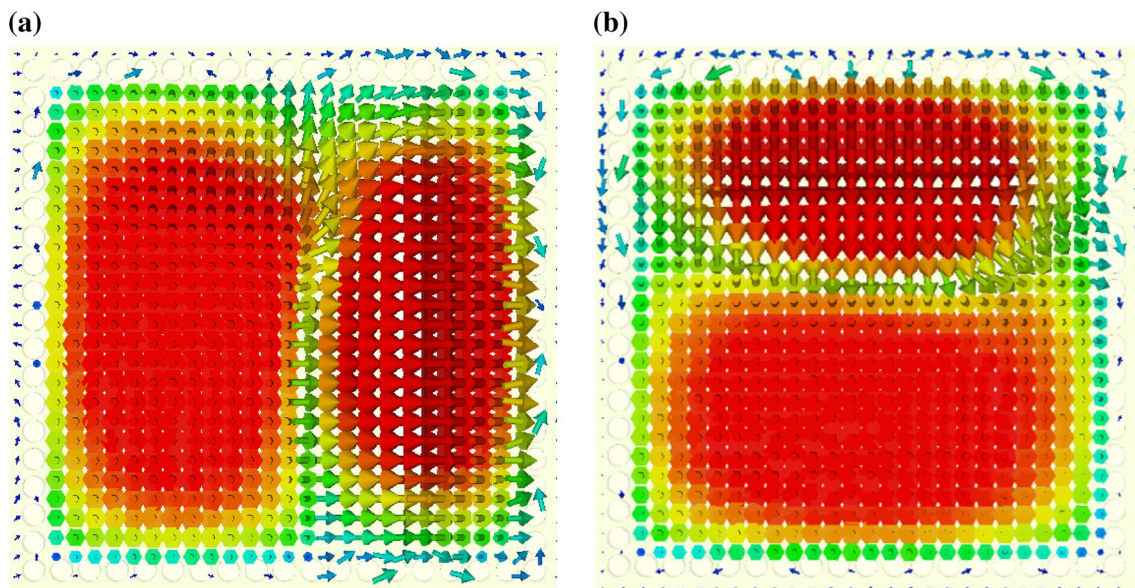


Fig. 3 Vertical view of the electric field distributions for the presented SIW-based polarization converter at the resonant frequency of 7.34 GHz. **a** TM_{120} mode and **b** TM_{210} mode

converted into the x-polarized radiation after transmitting through the three layers slot-structures integrated with SIW cavity.

Next, the physical mechanism of the cross polarization conversion is discussed for the SIW-based polarizer based on the Fabry–Pérot cavity theory [35]. For convenience, the three layers of the proposed polarization converter were marked as M1, M2 and M3, respectively, just as shown in Fig. 1. In our design, the three-layer structures can form two isolated Fabry–Pérot-like resonant cavities: the first Fabry–Pérot-like resonant cavity constituted the layer M1 and M2, and the second Fabry–Pérot-like resonant cavity constituted the layer M2 and M3. The electric field distributions of the two resonant cavities are shown in Fig. 5a, b. The incident wave can be either u-polarized or v-polarized and the resonant frequency of 7.34 GHz is considered.

From Fig. 5a, b, the incident EM wave comes into the first Fabry–Pérot-like resonant cavity and travels back and front in between M1 and M2. The polarization of the transmission wave is thereby rotated by 135° due to the multiple polarization couplings. Subsequently, the polarization of the transmission wave is further rotated by about 135° when it penetrates through the second Fabry–Pérot-like resonant cavity. As a consequence, the y-polarized incident wave is efficiently transmitted to x-polarized wave. Considering that the designed structure is sensitive to polarization, the transmission of co-polarization and cross-polarization is zero for the case of the x-polarized incidence. Due to SIW cavity resonance effect, the efficiency of the transmission polarization conversion has been greatly improved at the resonance

frequency of 7.34 GHz. In the next discussion, we will focus on the case of SIW cavity resonance.

4 Experimental results

To experimentally verify the performance of the proposed SIW-based polarization converter, we fabricated the structure with the dimension $200\text{ mm} \times 200\text{ mm}$ as shown in Fig. 6, containing 10×10 unit cells. The overall structural image, vertical view and top view of the experimental sample are shown in Fig. 6a–c, respectively. The method we have adopted is the traditional printed circuit board (PCB) techniques. The measurements were performed using an Agilent N5230A vector network analyzer and two broadband horn antennas [36], and the image of the experimental setup is shown in Fig. 6d.

Figure 7 shows the cross-polarization transmission coefficients of the proposed SIW-based polarization converter for the y-polarization incidence waves, the solid and dash-dotted line are simulated and measured results, respectively. For comparison, the simulation result shown in Fig. 2 is also presented again. From Fig. 7, we can observe that the measured cross-polarization transmission t_{xy} is in good agreement with the simulation. The simulated and measured results demonstrate that the linear y-polarization wave can be completely converted to its cross-polarization at the resonant frequency, and then transmitted. The tiny discrepancy is caused by the fabrication error and the un-negligible loss in the Teflon substrate.

Fig. 4 Electric field distributions at different positions in $-z$ direction, **a–f** y-polarized wave, **h–m** x-polarized wave

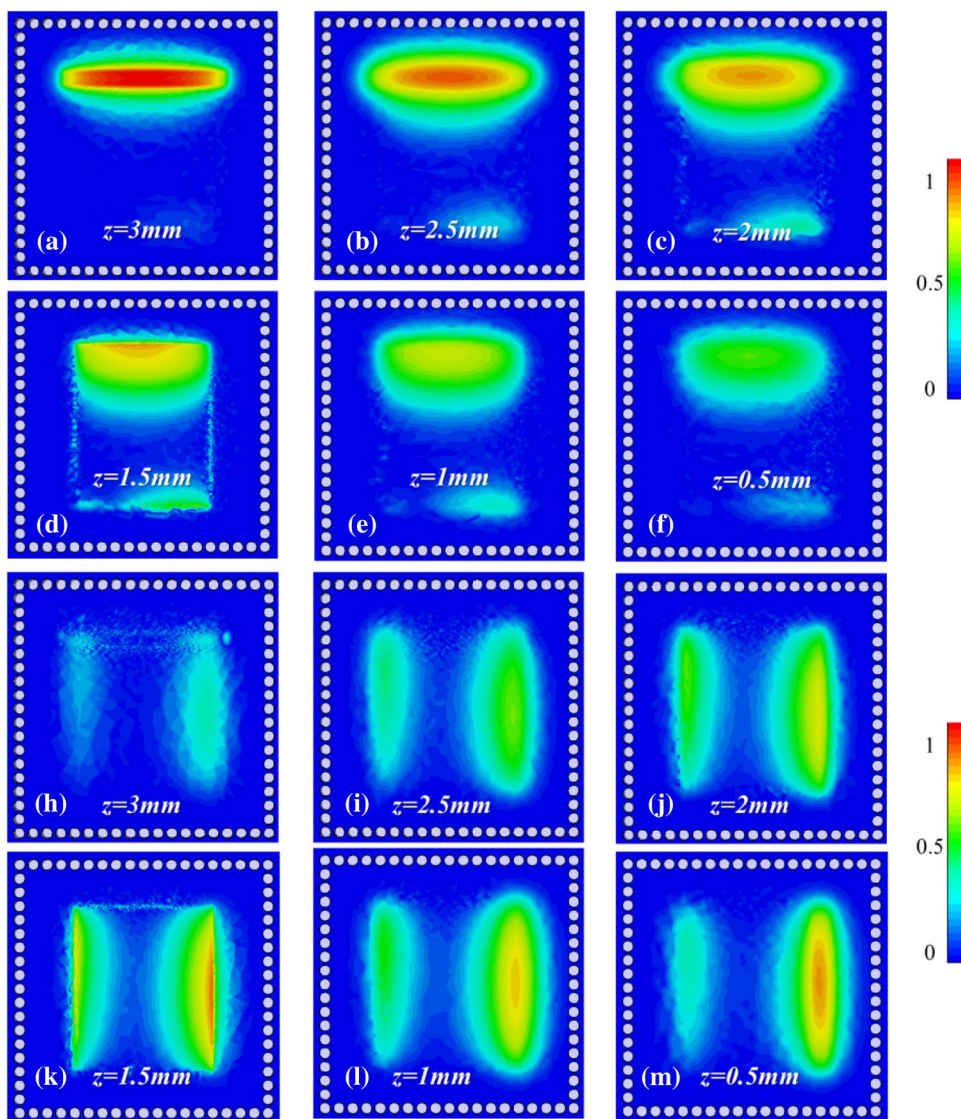


Fig. 5 **a** Electric field distribution for the first Fabry–Pérot-like resonance cavity; **b** electric field distribution for the second Fabry–Pérot-like resonance cavity

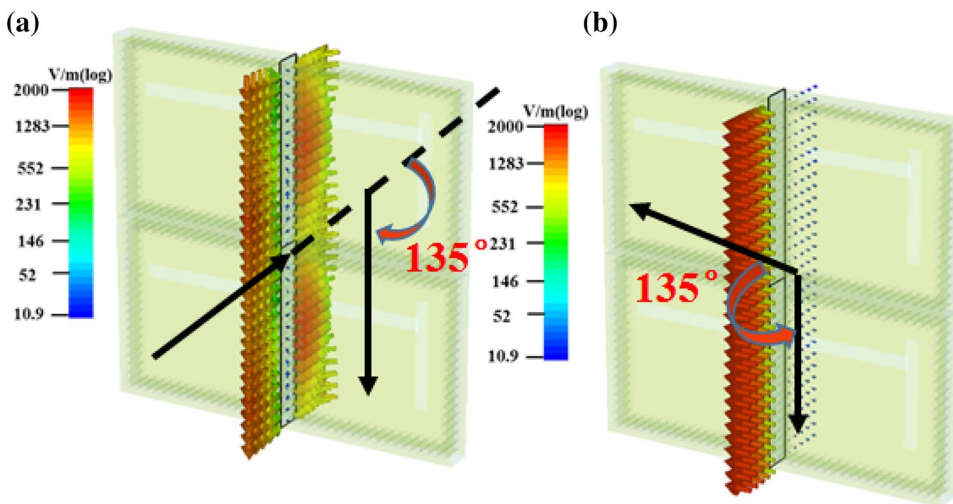


Fig. 6 Photograph of the fabrication SIW-based polarizer. **a** Overall structural diagram of the experimental sample, **b** vertical view of the experimental sample, **c** top view of the experimental sample and **d** image of the utilized experimental setup

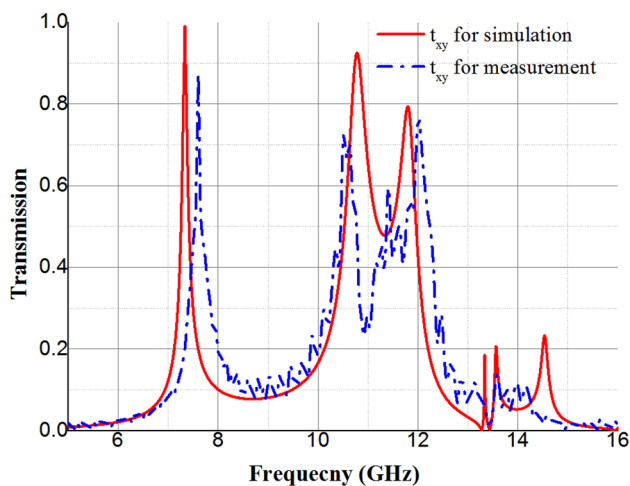
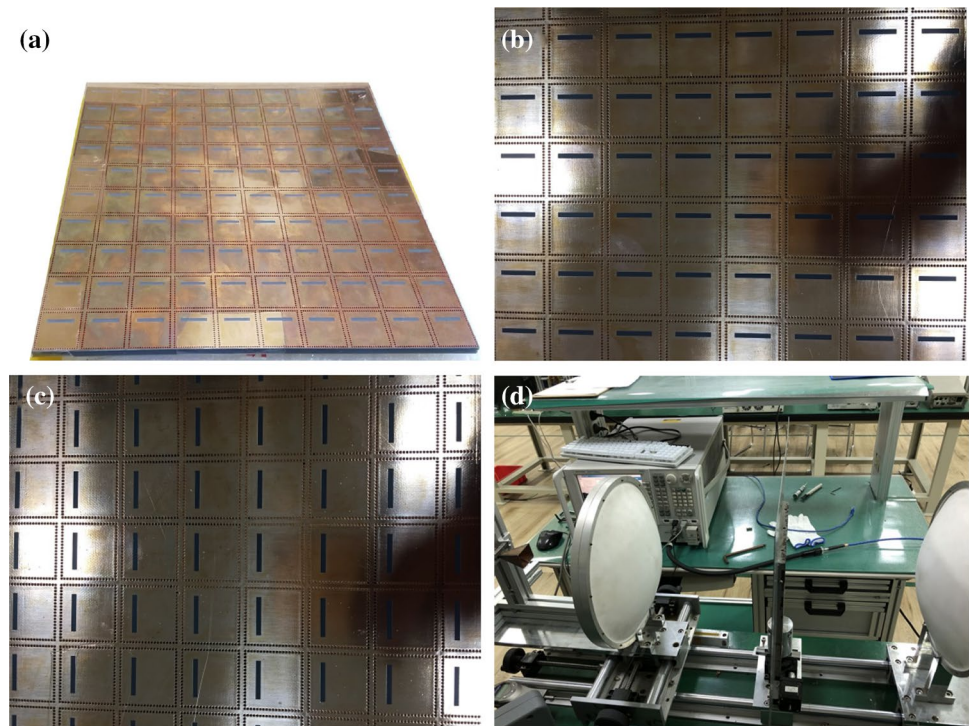


Fig. 7 Cross-polarization transmission characteristics of the proposed SIW-based polarizer, solid line for simulation, and dash-dotted line for experiment

5 Conclusions

In conclusion, the three-layer transmission polarization converter based on the SIW technology has been put forward and proved both numerically and experimentally. The proposed SIW-based polarizer can accomplish perfect polarization conversion with near 1 of polarization conversion efficiency at the resonance frequency of 7.34 GHz.

For verifying our design, we fabricated the SIW-base polarizer with 10×10 basic elements. By comparing the measurement and the simulations, it proves that the novel transmission polarizer with high-efficiency polarization conversion can be realized by integrating with the SIW cavity. The electric field distributions in the resonance cavities are discussed for revealing the underlying physical mechanisms of the high-efficiency polarization conversion, and higher-order modes (such as TM_{120} , TM_{210}) in the SIW cavity play an important role in improving the polarization conversion efficiency. Furthermore, the specific changing process of electric field in x- and y-directions is analyzed in detail, which is intuitively characterized by the process of converting a linearly polarized wave into its orthogonal polarized ones. The transmission polarization converter is expected to be employed in many applications such as asymmetric radome.

Acknowledgements This research was partially supported by the National Natural Science Foundation of China (Grant No. 51301031), and Supported by Program for Changjiang Scholars and Innovative Research Team in University (PCSIRT).

References

1. N.I. Landy, S. Sajuyigbe, J.J. Mock et al., Perfect metamaterial absorber. *Phys. Rev. Lett.* **100**(20), 207402 (2008)

2. N. Fernez, L. Burgnies, J. Hao et al., Radiative quality factor in thin resonant metamaterial absorbers. *IEEE Trans. Microw. Theory Tech.* **66**(4), 1764–1772 (2018)
3. D. Schurig, J.J. Mock, B.J. Justice et al., Metamaterial electromagnetic cloak at microwave frequencies. *Science* **314**(5801), 977–980 (2006)
4. S.S. Islam, M.M. Hasan, M.R.I. Faruque, A new metamaterial-based wideband rectangular invisibility cloak. *Appl. Phys. A* **124**(2), 160 (2018)
5. J. Chen, H. Yang, G. Zhang et al., Integrating an ultra-broadband power splitter and a polarization converter using a zigzag metamaterial. *Opt. Mater. Express* **8**(6), 1454–1462 (2018)
6. X. Gao, L. Singh, W. Yang et al., Bandwidth broadening of a linear polarization converter by near-field metasurface coupling. *Sci Rep* **7**(1), 6817 (2017)
7. R. Zhao, H.Y. Chen, L. Zhang et al., Design and implementation of high efficiency and broadband transmission-type polarization converter based on diagonal split-ring resonator. *Prog. Electromagn. Res.* **161**, 1–10 (2018)
8. S.Y. Wang, W. Liu, W. Geyi, Dual-band transmission polarization converter based on planar-dipole pair frequency selective surface. *Sci. Rep* **8**(1), 3791 (2018)
9. B. Gerislioglu, A. Ahmadvand, M. Karabiyik et al., VO₂-based reconfigurable antenna platform with addressable microheater matrix. *Adv. Electron. Mater.* **3**(9), 1700170 (2017)
10. Y. Liu, K. Li, Y. Jia et al., Wideband RCS reduction of a slot array antenna using polarization conversion metasurfaces. *IEEE Trans. Antennas Propag.* **64**(1), 326–331 (2016)
11. F. Khosravi, P. Mousavi, Bidirectional same-sense circularly polarized slot antenna using polarization converting surface. *IEEE Antennas Wirel. Propag. Lett.* **13**, 1652–1655 (2014)
12. M. Jusoh, T. Sabapathy, M.F. Jamlos et al., Reconfigurable four-parasitic-elements patch antenna for high-gain beam switching application. *IEEE Antennas Wirel. Propag. Lett.* **13**, 79–82 (2014)
13. P.C. Kim, W.G. Lim, I.S. Seo, Polarization characteristics of a composite stealth radome with a frequency selective surface composed of dipole elements. *Compos. Struct.* **90.2**, 242–246 (2009)
14. A. Parsa, T. Kodera, C. Caloz, Ferrite based non-reciprocal radome, generalized scattering matrix analysis and experimental demonstration. *IEEE Trans. Antennas Propag.* **59**(3), 810–817 (2011)
15. B. Gerislioglu, A. Ahmadvand, N. Pala, Single-and multimode beam propagation through an optothermally controllable Fano clusters-mediated waveguide. *J. Lightwave Technol.* **35**(22), 4961–4966 (2017)
16. B. Gerislioglu, A. Ahmadvand, N. Pala, Tunable plasmonic toroidal terahertz metamodulator, *Phys. Rev. B*, 97(16), 161405
17. T. Kaelberer, V.A. Fedotov, N. Papasimakis et al., Toroidal dipolar response in a metamaterial. *Science* **330**(6010), 1510–1512 (2010)
18. B. Gerislioglu, A. Ahmadvand, N. Pala, Functional quadrumer clusters for switching between Fano and charge transfer plasmons. *IEEE Photonics Technol. Lett.* **29**(24), 2226–2229 (2017)
19. W. Liu, S. Chen, Z. Li et al., Realization of broadband cross-polarization conversion in transmission mode in the terahertz region using a single-layer metasurface. *Opt. Lett.* **40**(13), 3185–3188 (2015)
20. D. Sui, H. Ma, J. Wang et al., Symmetry-based coding method and synthesis topology optimization design of ultra-wideband polarization conversion metasurfaces. *Appl. Phys. Lett.* **109**(1), 014104 (2016)
21. N.K. Grady, J.E. Heyes, D.R. Chowdhury et al., Terahertz metamaterials for linear polarization conversion and anomalous refraction. *Science* **340**(6138), 1304–1307 (2013)
22. K. Chen, Y. Feng, F. Monticone et al., A reconfigurable active Huygens' metalens. *Adv. Mater.* **29**(17), 1606422 (2017)
23. K. Chen, Y. Feng, L. Cui et al., Dynamic control of asymmetric electromagnetic wave transmission by active chiral metamaterial. *Sci. Rep.* **7**, 42802 (2017)
24. D. Deslandes, K. Wu, Accurate modeling, wave mechanisms, and design considerations of a substrate integrated waveguide. *IEEE Trans. Microw Theory Tech.* **54**(6), 2516–2526 (2006)
25. M. Bozzi, A. Georgiadis, K. Wu, Review of substrate-integrated waveguide circuits and antennas. *IET Microw. Antennas Propag.* **5**(8), 909–920 (2011)
26. M. Barbuto, F. Bilotti, A. Toscano, Linear-to-circular polarization transformer using electrically small antennas, in *Proceedings of the 2012 IEEE International Symposium on Antennas and Propagation*, 1–2(2012)
27. M. Barbuto, F. Trotta, F. Bilotti et al., Filtering chiral particle for rotating the polarization state of antennas and waveguides components. *IEEE Trans. Antennas Propag.* **65**(3), 1468–1471 (2017)
28. X. Ma, C. Huang, W. Pan et al., A dual circularly polarized horn antenna in Ku-band based on chiral metamaterial. *IEEE Trans. Antennas Propag.* **62**(4), 2307–2311 (2014)
29. M. Barbuto, F. Trotta, F. Bilotti et al., Design and experimental validation of dual-band circularly polarized horn filtenna. *Electron. Lett.* **53**(10), 641–642 (2017)
30. Y. Li, Y. Pang, J. Wang et al., Wideband polarization conversion with the synergy of waveguide and spoof surface Plasmon polariton modes. *Phys. Rev. Appl.* **10**(6), 064002 (2018)
31. J. Wang, W. Wu, Cavity-based linear-to-circular polarization converter. *Opt. Exp.* **25**(4), 3805–3810 (2017)
32. S.A. Winkler, W. Hong, M. Bozzi et al., Polarization rotating frequency selective surface based on substrated waveguide technology. *IEEE Trans. Antennas Propag.* **58**(4), 1202–1213 (2010)
33. CST, Microwave studio. <http://www.cst.com>
34. F.X. Li, H.Y. Chen, Q.T. He et al., Design and implementation of metamaterial polarization converter with the reflection and transmission polarization conversion simultaneously, *J. Opt.* (2019) (**in press**)
35. R. Sauleau, in *Fabry Perot resonators, Encyclopedia of RF and Microwave Engineering*, 2, ed. by K. Chang (Wiley, New York, 2005), pp. 1381–1401
36. H.Y. Chen, H.B. Zhang, L.J. Deng, Design of an ultra-thin magnetic-type radar absorber embedded with FSS. *IEEE Antennas Wirel. Propag. Lett.* **9**, 899–901 (2010)

Publisher's Note Springer Nature remains neutral with regard to jurisdictional claims in published maps and institutional affiliations.